Editor's Summary

Going with the Flow … or Not

In healthy people, blood flows freely throughout the body, delivering oxygen to tissues via the molecule hemoglobin. For those with sickle cell disease, red blood cells carry a mutated form of hemoglobin, called hemoglobin S, that changes cells into a rigid sickle, or crescent, shape and causes blood flow to slow markedly. Although sickle cell disease can be detected through genetic and molecular tests, there is no objective biomarker of clinical outcome. Wood *et al.* therefore devised a microfluidic device that can mimic this vaso-occlusive event, allowing them to detect biophysical changes in blood —a new type of marker that could stratify sickle cell patients on the basis of disease severity.

Wood *et al.* collected blood from 29 patients: 23 of which were classified as having "severe" disease, and 6 of which were "benign." The blood was flowed through a microfluidic device consisting of a channel coupled to an oxygen reservoir. As sickle cells become deoxygenated, they adopt their stiff, sickle shape. In their device, such deoxygenation would result in a drop in flow velocity, which could be measured as a change in conductance. This biophysical marker helped the authors to successfully identify benign versus severe samples, without using less reliable markers like white blood cell count and hemoglobin S fraction. Wood and colleagues could also predict a patient's response to therapy, such as a blood transfusion or small-molecule drugs.

It may never be possible to predict the exact timing of vaso-occlusion, but the ex vivo biophysical test proposed by Wood *et al.* can objectively identify patients who are not responding well to treatment or transfusion. Conversely, the test could pinpoint those who may benefit from such therapies, putting more patients on treatment regimens that make their red blood cells just go with the flow.

SICKLE CELL DIAGNOSTICS

A Biophysical Indicator of Vaso-occlusive Risk in Sickle Cell Disease

David K. Wood,[1] Alicia Soriano,[2] L. Mahadevan,[3,4]* John M. Higgins,[4,5]* Sangeeta N. Bhatia[1,6,7]

The search for predictive indicators of disease has largely focused on molecular markers. However, biophysical markers, which can integrate multiple pathways, may provide a more global picture of pathophysiology. Sickle cell disease affects millions of people worldwide and has been studied intensely at the molecular, cellular, tissue, and organismal level for a century, but there are still few, if any, markers quantifying the severity of this disease. Because the complications of sickle cell disease are largely due to vaso-occlusive events, we hypothesized that a physical metric characterizing the vaso-occlusive process could serve as an indicator of disease severity. Here, we use a microfluidic device to characterize the dynamics of "jamming," or vaso-occlusion, in physiologically relevant conditions, by measuring a biophysical parameter that quantifies the rate of change of the resistance to flow after a sudden deoxygenation event. Our studies show that this single biophysical parameter could be used to distinguish patients with poor outcomes from those with good outcomes, unlike existing laboratory tests. This biophysical indicator could therefore be used to guide the timing of clinical interventions, to monitor the progression of the disease, and to measure the efficacy of drugs, transfusion, and novel small molecules in an ex vivo setting.

INTRODUCTION

Biomarkers for disease are critical to guide clinical intervention and to speed up the development of new therapies. The search for such markers has yielded many new genetic, epigenetic, and proteomic indicators (1–5); yet, the need for new markers continues to outpace their clinical validation and use (6). This problem is particularly acute for some diseases, such as sickle cell disease, where no molecular markers have been found to correlate reliably with the clinical outcomes (7–10). Markers that provide integrative systemic assessments are complementary to molecular indicators; for example, biophysical markers are already used clinically and range from long-standing measurements, such as blood pressure, to newer imaging modalities, such as Doppler ultrasound and cerebral flow magnetic resonance imaging (11–13). Because these biophysical metrics integrate multiple-length scales, molecules, and pathways, they have the potential to reflect disease state more accurately than their molecular counterparts. Even at the cellular scale, recent studies suggest new possibilities for biophysical markers, such as cell motility or cell deformability, as an important indicator of metastatic potential in cancer (14, 15) and other diseases (16, 17).

Sickle cell disease, which affects more than 13 million people worldwide (18) and costs more than $1.1 billion per year in the United States alone (19), is an ideal candidate for a biophysical indicator. The molecular origin of the disease is a mutation in the gene encoding the β-globin protein that results in a variant hemoglobin molecule [hemoglobin S (HbS)]. HbS polymerizes into long chains and extended gels upon deoxygenation (20, 21), leading to the formation of stiff and often sickle-shaped red blood cells (RBCs). Sickle cells cause changes in blood flow, which can lead to clinical vaso-occlusive "crisis" events (22). Although the molecular origin of sickle cell disease has been known for more than 60 years (23), the factors and processes that link these molecular and cellular events to clinical outcomes in patients remain elusive (24–26). The search for mechanism is particularly challenging because pathogenesis of vaso-occlusion involves several processes across multiple length and time scales, including polymerization and melting of hemoglobin, stiffening and morphological change of RBCs, and increasing apparent viscosity of blood. Each of these processes has been examined separately in various in vitro systems (20, 21, 27–30). However, studies that integrate all of these processes in physiologic regimes are rare, even though their combined effects likely determine clinical outcomes (28, 31–32).

In the absence of objective biomarkers of disease severity (7–10), it is difficult to predict the frequency of painful and damaging vaso-occlusive crises and overall severity of disease for individual patients. Common laboratory tests measure HbS fraction and fetal hemoglobin (HbF) fraction, neither of which is predictive of clinical outcome for individual patients (9, 33). Thus, we have no method to predict which patients will require urgent or frequent treatment (8, 10), and it is difficult to assess efficacy of different treatments. This lack of clear predictors also confounds the development of new therapeutics because we have no reliable in vitro methods to test which molecules are most likely to work in vivo (22). Because the morbidity and mortality are caused by vaso-occlusions (34), a biophysical marker might provide a link to clinical phenotype. For example, in vivo cerebral blood flow velocity measurements have shown value in guiding transfusion therapy for pediatric sickle cell patients (35–37), suggesting that it may be possible to translate the extensive research on biophysical aspects of sickle cell disease (38) into an in vitro biophysical marker.

Recent studies have shown that it is possible to halt the flow of sickle cell blood in a capillary-sized microchannel under constant pressure by lowering the oxygen concentration, thereby simulating

[1]Division of Health Sciences and Technology, Massachusetts Institute of Technology, Cambridge, MA 02139, USA. [2]Special Hematology Laboratory, Brigham and Women's Hospital, Boston, MA 02115, USA. [3]School of Engineering and Applied Sciences, Department of Physics, Department of Organismic and Evolutionary Biology, Wyss Institute for Biologically Inspired Engineering and Kavli Institute for Nanobio Science and Technology, Harvard University, Cambridge, MA 02138, USA. [4]Department of Systems Biology, Harvard Medical School, Boston, MA 02115, USA. [5]Center for Systems Biology and Department of Pathology, Massachusetts General Hospital, Boston, MA 02114, USA. [6]Howard Hughes Medical Institute, Department of Electrical Engineering and Computer Science and Koch Institute for Integrative Cancer Research, Massachusetts Institute of Technology, Cambridge, MA 02139, USA. [7]Division of Medicine, Brigham and Women's Hospital, Boston, MA 02115, USA.
*To whom correspondence should be addressed. E-mail: lm@seas.harvard.edu (L.M.); john_higgins@hms.harvard.edu (J.M.H.)

the most basic features of a vaso-occlusive event (*39, 40*). Here, we show that a measurement of the dynamics of the integrated physical vaso-occlusive process using patient blood ex vivo serves as a biophysical indicator of pathophysiology in a physiologically relevant range of HbS concentration, HbS fraction, RBC volume fraction, and local oxygen concentration (*28*). This measurement characterizes the dynamics of blood rheological properties during ex vivo vaso-occlusion. Our experiments evaluated this measurement as a biophysical indicator of disease severity in patients, by benchmarking it against currently available clinical laboratory tests for sickle cell disease, and as an ex vivo assessment of the efficacy of existing and experimental treatments.

RESULTS

A microfluidic system quantifies blood conductance dynamics

We developed a microfluidic system to measure changes in sickle cell blood flow after deoxygenation. The system included a microfluidic device with a capillary-sized channel that was diffusively coupled to a gas reservoir (Fig. 1A). This system allowed control over many parameters that mimic physiological conditions during vaso-occlusion, including channel size, blood pressure, and oxygen concentration. Whole, anticoagulated human blood was driven through the channel under constant pressure, and gas with prescribed oxygen concentration was driven through the gas reservoir. RBCs were imaged in the Soret band (*41*), allowing determination of hemoglobin oxygenation state on the basis of change in optical absorption (Fig. 1B). As sickle cells become deoxygenated, hemoglobin polymerizes, leading to cell stiffening and sickling. In the microfluidic device, there was thus an accompanying increase in the blood's resistance to flow, with a resulting drop in flow velocity despite a constant driving pressure head; that is, there was a drop in the blood conductance (defined as velocity per unit pressure drop, and inversely proportional to the effective viscosity of the suspension).

By measuring the changes in flow velocity for a given constant applied pressure head, we could quantify the kinetics of the change in conductance for a blood sample after deoxygenation (Fig. 2). Movie S1 shows a full deoxygenation-reoxygenation cycle with vaso-occlusion and recovery. When the oxygen concentration in the gas reservoir was reduced rapidly from 21 to 0% in ~20 s (Fig. 2, A to F, top panels), it caused hemoglobin desaturation (fig. S1), cell deoxygenation, cell stiffening, and an overall decrease in blood flow velocity in blood samples from patients with sickle cell disease, although the pressure drop across the device remained unchanged (Fig. 2, C to F, middle panels, right *y* axis). In contrast, blood samples from individuals with either normal hemoglobin A (HbA) (Fig. 2A) or sickle cell trait (heterozygous for the mutated β-*globin* gene) (Fig. 2B) showed no response. For all blood samples, steady-state velocity at 21% oxygen also depended linearly on the pressure drop, consistent with Poiseuille's law (*42*), with maximum shear rates in the middle of the channel in the range of 100 to 400 s^{-1}, which are similar to shear rates found in the microcirculation in vivo (*43*). For sickle cell patient blood, deoxygenation was followed by a declining velocity with the magnitude of deceleration varying roughly linearly with applied pressure. That is, the rate of decrease in conductance was independent of pressure (Fig. 2, C to F, bottom panels). We therefore used the rates of conductance decrease in blood samples from different sickle cell patients as measures of disease severity.

Conductance dynamics correlate with clinical outcome

If the rate of conductance decrease captures critical aspects of in vivo sickle cell pathophysiology, then we hypothesized that blood samples from the most severely affected patients would show a more rapid reduction in conductance ($\Delta C/\Delta t$) than samples from the least severely affected (benign) patients. To test this hypothesis, we defined criteria to distinguish "benign" and "severe" blood samples. A benign sample was one collected from a sickle cell patient who had not been treated with hydroxyurea, had not received any transfusions, and had no impromptu medical visits for a sickle cell disease–related indication in
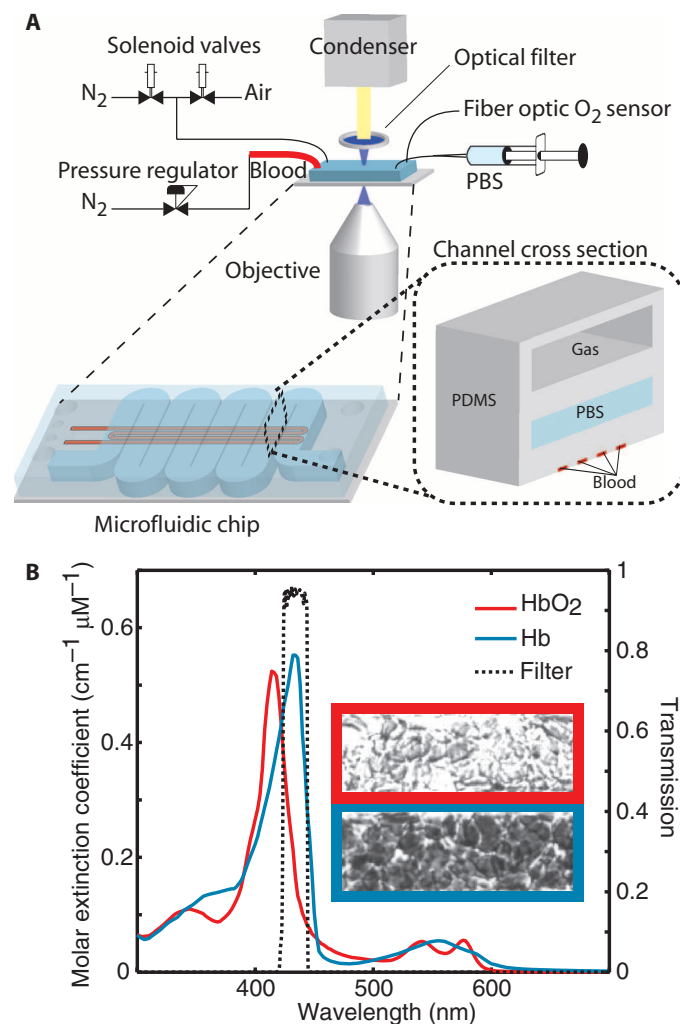

Fig. 1. Microfluidic device for studying sickle cell blood flow conductance. (**A**) The device comprised three layers (inset): artificial capillaries for blood flow, a hydration layer with PBS, and a gas reservoir. Blood was driven under constant pressure bias, controlled by a digital pressure regulator. Two solenoid valves controlled the gas (N$_2$ and air) in the top chamber. A fiber optic probe was used to measure the oxygen concentration in the gas reservoir. The device was illuminated through an optical filter whose transmission band (434 ± 17 nm) was centered on an absorption peak for deoxyhemoglobin. (**B**) The absorption peak of hemoglobin shifts in deoxygenated conditions, making deoxygenated RBCs appear dark and oxygenated RBCs appear transparent. Qualitative measurements of hemoglobin oxygen saturation were made using the intensity of transmitted light.

the 12 months before or 2 months after the date of sample collection. Benign blood samples showed little or no drop in conductance after deoxygenation (Fig. 3A). Severe samples were those from sickle cell patients who had either received a transfusion or made an impromptu hospital visit for a sickle cell disease–related indication in the 12 months before or 2 months after the date of sample collection. Samples from patients with severe disease showed a steep and rapid conductance change after deoxygenation (Fig. 2, C to F, and 3B).
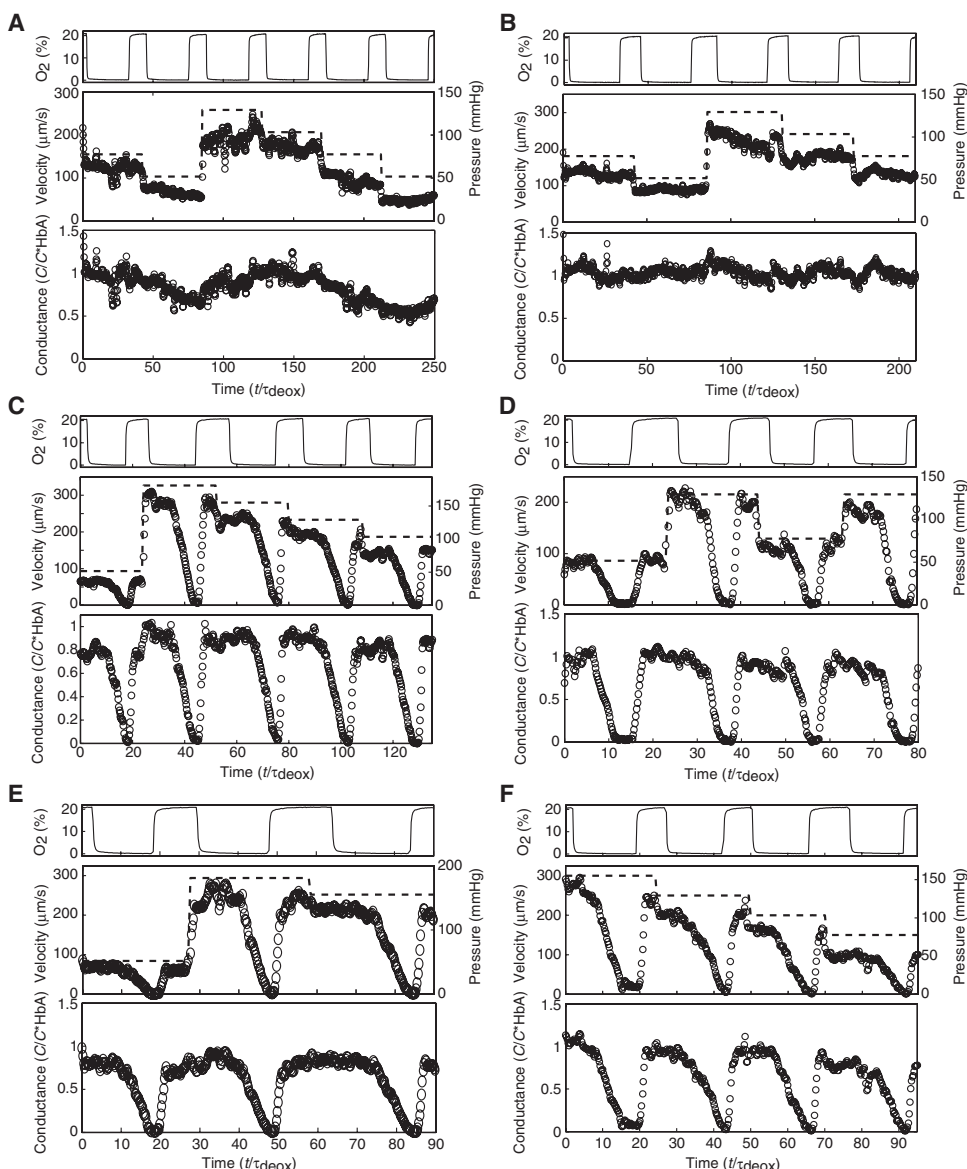
Conductance dynamics efficiently stratify sickle cell patients

Tests were carried out with blood samples from 23 patients with severe disease and 6 patients with benign disease. Deoxygenation tests indicated that the rate of conductance decrease correlated with benign and severe classification for this set of blood samples, averaged over at least three independent deoxygenation experiments (Fig. 4). Table S1 contains raw data for all samples. Blood samples from patients with more benign disease showed a significantly slower decrease in the conductance after deoxygenation (Fig. 4A): the conductance of the median severe sample fell more than twice as fast as that of the median benign sample.

We also calculated the receiver operating characteristic (ROC), which characterizes the sensitivity and specificity for a binary test as a function of the discrimination threshold, and the area under the curve (AUC), which quantifies the ability of the test to discriminate between states (6, 44). In contrast to a random prediction (Fig. 4B, dashed line), which has no information content, our measurement (Fig. 4B, solid line) demonstrated strong diagnostic potential with an AUC of 0.85 (95% confidence level = 0.65 to 0.95).

We explored the possibility that these different rates of conductance change could be explained by other blood parameters. No systematic difference was noted between the benign and the severe groups for HbS fraction (Fig. 4C), unadjusted hematocrit (Fig. 4E), mean hemoglobin concentration (fig. S2A), sample storage time (fig. S2B), or steady-state oxygenated conductance (Fig. 4F). We also considered the role of white blood cells (WBCs) and found no correlation between sample severity and WBC count (Fig. 4D). We expect that most WBCs are not viable at the time of testing, and thus, WBCs are not responsible for the differences in rheodynamics. We further explored this hypothesis by depleting WBCs from a severe sample and showed that the rheodynamics were not consistently altered (fig. S2C); thus, none of these other blood parameters can serve as a predictive biomarker for disease severity.

Another potential explanation for these different rates of conductance change is that the benign group has a higher fraction of HbF, which inhibits HbS polymerization (45). To compare HbF fractions between the benign and the severe samples, we first subdivided the severe samples into those from patients who had been or had not been treated with hydroxyurea ("treated severe" or "untreated severe"), a drug that works in part by increasing HbF expression
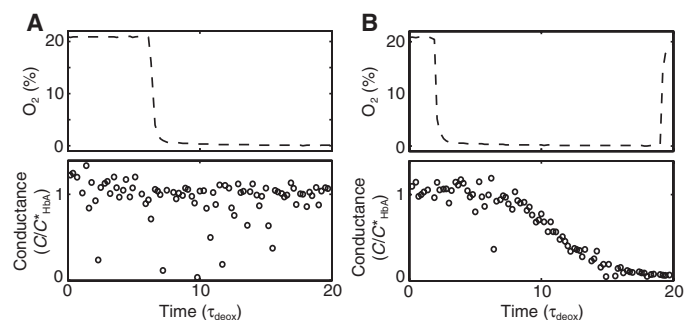
Fig. 2. Measuring rates of conductance decrease after deoxygenation. (**A**) A normal blood sample. (**B**) A sickle trait blood sample. (**C** to **F**) Severe sickle cell samples from four individual patients. For each sample, measurements show time courses of oxygen concentration (top panels) in the gas reservoir and corresponding RBC median velocity (middle panels, open circles) obtained by video tracking, as well as applied pressure bias (middle panels, dashed line). Corresponding channel conductance (bottom panels) was measured by dividing instantaneous velocity (μm/s) by the pressure (mmHg). All conductance values were scaled by the mean HbA blood conductance [$C^*_{HbA} = 1.7\ \mu m\ s^{-1}\ mmHg^{-1}$ (0.013 $\mu m\ s^{-1}\ Pa^{-1}$)]. Time was scaled by the time course for hemoglobin deoxygenation ($\tau_{deox} = 10$ s).

Fig. 3. Rheodynamics for severe and benign samples. (**A** and **B**) Oxygen concentration in the gas reservoir and corresponding conductance data for one benign sample (A) and one severe sample (B). This figure shows one deoxygenation cycle from a series of such cycles as shown in Fig. 2. All conductance values are scaled by the mean HbA blood conductance [~1.7 $\mu m\ s^{-1}\ mmHg^{-1}$ (0.013 $\mu m\ s^{-1}\ Pa^{-1}$)], and time is scaled by the time scale for hemoglobin deoxygenation (~10 s).

(45, 46). Benign blood samples had higher HbF fractions than untreated severe samples (Fig. 4G). However, the HbF fractions for treated severe samples were comparable to those for the benign samples. Despite elevated HbF fraction, the hydroxyurea-treated patients had a more severe clinical course, and their blood samples showed rates of conductance decrease comparable to those of untreated severe samples (Fig. 4H). Although increased HbF fraction may account for some of the difference in $\Delta C/\Delta t$ between benign samples and untreated severe samples, HbF fraction cannot account for the difference between the benign and the treated severe samples. Further, if HbF fraction alone determined the rheodynamics, then one would not expect the untreated and treated severe samples to show such similar rates of conductance decrease.

Finally, we also assessed the role of cell volume by comparing the mean cell volumes (MCVs) in the groups. Hydroxyurea is known to raise MCVs, and we found a slight elevation in MCVs in the hydroxyurea-treated group, as expected (fig. S2D). We found no significant difference between the benign and the untreated severe groups, making it unlikely that differences in RBC volume are responsible for the differences in rheodynamics.

Simulated transfusion reduces rates of conductance change

We investigated whether a simulated transfusion of normal blood (HbA) to lower HbS fraction would lead to slower declines in conductance, analogous to the way that it improves sickle cell patient clinical status (46). We mixed ABO- and RhD-compatible HbA blood with blood samples from four sickle cell patients. After a simulated transfusion, the HbS fraction of four severe samples was reduced by 29, 31, 33, or 35% (Fig. 4I). As expected, lower HbS fraction is associated with slower conductance decreases for each sample. Despite the similarity in relative reduction of HbS fraction, the magnitude of the effect on conductance was variable between patients; as such, neither the initial HbS fraction nor the fractional decrease seems to predict how the rheological properties of a given blood sample will respond.

Small-molecule treatment modulates rate of conductance change

If the rate of conductance decrease correlates with clinical outcome, small molecules with clinical potential should reduce the rate of conductance decrease. Recent work has described a small molecule, 5-hydroxymethyl furfural (5HMF), that increases hemoglobin oxygen affinity and can significantly improve phenotypes in a mouse model of sickle cell disease (47). We used our system to assess the effect of this experimental therapy on the rheological properties of a patient blood sample ex vivo. One patient sample was treated with either 0 mM 5HMF (untreated) or 10 mM 5HMF. The results showed a large and rapid conductance decrease in response to deoxygenation for the untreated sample (Fig. 5A), but little conductance change for the treated sample (Fig. 5B). Treatment with 5HMF caused a fivefold slower reduction in conductance compared to the untreated sample (Fig. 5C). This marked rheodynamic response was associated with a slower change in the optical absorption measurement (Fig. 5A, top panel) compared to that for the untreated sample (Fig. 5B, top panel), consistent with a slower unloading of oxygen for the treated sample.

DISCUSSION

Our microfluidic system enabled us to measure the speed of the rheological response of patient blood samples to deoxygenation by integrating the molecular, cellular, and rheological processes that likely occur during in vivo vaso-occlusion. This method contrasts with previous approaches that have focused on just one aspect of the vaso-occlusive process, such as HbS polymerization, RBC sickling, or blood rheology. We have shown that the rate of change in the rheological properties of blood samples—characterized by the rate of change in conductance during an in vitro vaso-occlusive event—is correlated with overall patient disease severity for the set of 29 patients in our study. The ability of this biophysical indicator to distinguish patient disease severity in this patient cohort was statistically robust ($P < 0.01$) with >90% statistical power (for $P = 0.05$). From a diagnostic perspective, our biophysical indicator, with an AUC of 0.85, compares well against other putative biomarkers deemed sufficiently promising for follow-up study, such as a micro-nuclear magnetic resonance (NMR)–based cancer diagnostic (AUC = 0.44 to 0.88) (48) and urinary biomarkers for kidney injury (AUC = 0.73 to 0.91) (49). This diagnostic efficiency contrasts sharply with existing laboratory tests such as HbS and HbF fractions, which do not correlate with patient outcomes (10, 50). Because we find less heterogeneity in rheodynamics for benign samples than for severe samples (Fig. 4A), this measurement may be most useful for identifying sickle cell patients at increased risk of vaso-occlusive complications as those with elevated rheodynamics. Although the sudden and seemingly unpredictable onset of vaso-occlusive crises suggests that it may never be possible to predict the exact timing of such events, our ex vivo biophysical test may provide the basis for an objective and accurate tool to identify those patients who are not responding well to hydroxyurea treatment or transfusion or who may benefit most from initiation of such treatment regimens.

Our study highlights the potential diagnostic power of a biophysical marker to integrate multiple interdependent pathophysiological processes, in contrast to previous studies at the molecular or cellular level (20, 21, 27–30). Furthermore, we see that a previously unappreciated difference between patients is found in the dynamics of blood rheological properties, reflecting the pathophysiological transition of a soft suspension that flows steadily to a "jammed" one when the cells stiffen in response to deoxygenation. Thus, it is not surprising that steady-state values, such as hematocrit, mean corpuscular volume, mean hemoglobin concentration, WBC count, and oxygenated conductance, do not correlate with clinical outcome, whereas the dynamics of flow

do correlate with the occlusive events ultimately responsible for disease severity. Indeed, more generally, stasis and hyperviscosity lead to thrombosis in vivo and thus imply a lower limit on physiologic steady-state velocity in the microcirculation (*51*). It is therefore not surprising that a key determinant of vaso-occlusion is the rate at which flow approaches this lower limit. In our measurements, the patients most at risk are those whose blood showed a rapid conductance change, indicating a high probability that it would slow sufficiently quickly in the microcirculation to reach pathologically low levels and produce a vaso-

occlusion. Understanding the occurrence of these extreme events requires a dynamic assay, such as that characterized here.

Animal models of sickle cell disease are limited by significant phenotypic differences from human patients and the complexity of experimental protocols (*7*). Our microfluidic approach may provide a better way to assess the efficacy of experimental pharmaceuticals in humans. The ex vivo system described in this study can be used to identify potential drugs and quantify their efficacy more easily by using only patient blood and obtaining a readout in fewer than 30 min. As an example, a reduced rate of conductance change after treatment of a blood sample with 5HMF (Fig. 5) was consistent with the known effects of this small molecule to increase hemoglobin oxygen affinity, slowing the kinetics of deoxygenation, and subsequent polymerization of HbS (*47*). Although this large increase in hemoglobin oxygen affinity may have been too large to allow release of oxygen to tissues in vivo, it is possible that a milder increase in hemoglobin oxygen affinity may be sufficient to alter flow dynamics in vitro and possibly in vivo.

Our results also help focus the question of why hydroxyurea treatment has such variable efficacy (*45*, *52*). Hydroxyurea is currently the only approved pharmaceutical treatment for sickle cell disease, and it works in part by increasing the HbF fraction (*10*, *45*, *53*). However, many patients treated with hydroxyurea show large increases in HbF fraction without significant clinical benefits. HbF is known to slow HbS polymerization and should therefore change the kinetics of RBC stiffening and blood conductance change (*45*). We found no consistent effect of total HbF fraction in a blood sample on the rate of conductance decrease after deoxygenation, consistent with previous studies showing that the fraction of HbF in treated patients is not a useful predictor of clinical outcomes in individual patients (*33*). One existing hypothesis to explain this result is that the degree of uniformity of the HbF distribution across all RBCs may be more important than the total fraction of HbF (*8*, *45*, *54*).

In summary, the strong correlation between blood rheodynamics and the clinical outcomes in our study population provides a valuable tool for scientific discovery, drug development, and possibly for patient monitoring and clinical decision-making in sickle cell disease. Our study is limited to a small cohort of patients and uses simplified criteria for the "severity" of the disease. Future studies are required to predict clinical course prospectively in
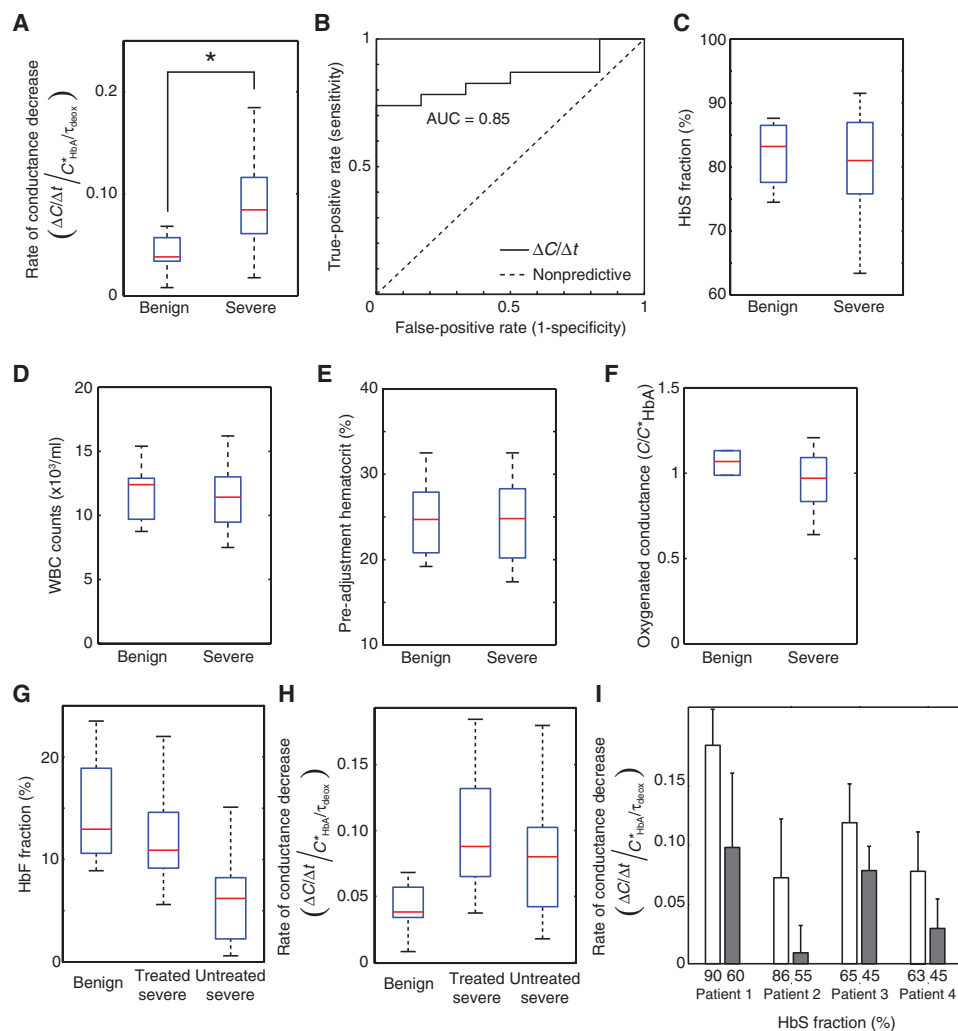

Fig. 4. Rate of conductance decrease correlates with patient clinical course. (**A**) Box plot comparing rates of conductance decrease for benign (*n* = 6) and severe samples (*n* = 23). *P < 0.01, Mann-Whitney nonparametric analysis. (**B**) ROC for rate of conductance decrease (solid line) and a theoretical random prediction (dashed line). (**C** to **F**) Box plots comparing HbS fraction, WBC count, hematocrit, and oxygenated conductance for benign and severe samples. (**G** and **H**) HbF fractions and rates of conductance change for benign and severe samples, further subdivided by hydroxyurea treatment. In box plots [(A) and (C) to (H)], the red line is the median, blue box shows interquartile range (IQR), and dashed lines show extent of data within 1.5-fold IQR. (**I**) Rates of conductance decrease for patient blood samples before and after addition of ABO- and RhD-compatible HbA blood, simulating a blood transfusion. Bar heights represent means, and error bars represent SDs of at least five deoxygenation cycles. Rates of conductance decrease are scaled by mean HbA blood conductance [~1.7 μm s^{-1} mmHg^{-1} (0.013 μm s^{-1} Pa^{-1})] divided by the time scale for hemoglobin deoxygenation (~10 s).
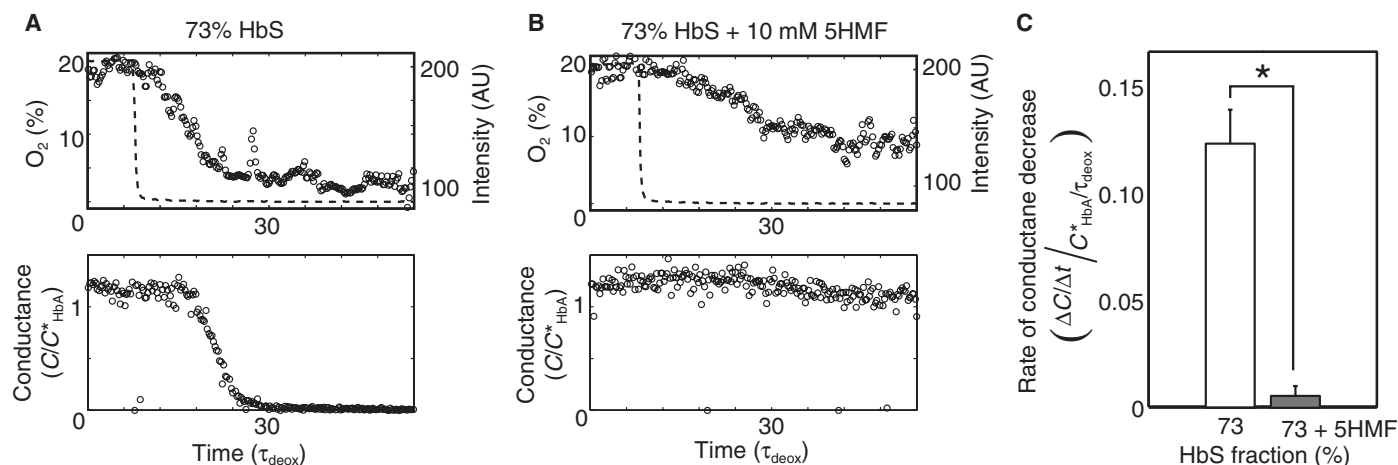
Fig. 5. Rate of conductance decrease is modulated by a small molecule. (**A** and **B**) Oxygen data from gas reservoir (top graph) and conductance data (bottom graph) are shown for an untreated severe sample (A) and the same sample treated with 10 mM 5HMF (B). Oxygen data are shown as measured in the gas reservoir (dashed line) and in the blood channel (open circles), the latter measured by RBC intensity. (**C**) Rates of conductance decrease [open circles in (A) and (B)] are quantified. *$P < 0.05$, Mann-Whitney nonparametric analysis. Data are means ± SD of at least five independent deoxygenation cycles for both samples. All conductance values are scaled by the mean HbA blood conductance [~1.7 μm s^{-1} mmHg^{-1} (0.013 μm s^{-1} Pa^{-1})], and time is scaled by the time scale for hemoglobin deoxygenation (~10 s). Rates of conductance decrease are scaled by mean HbA blood conductance divided by the time scale for hemoglobin deoxygenation (C^*_{HbA}/τ_{deox}).

larger populations and in individual patients longitudinally. This system could also be used to quantitatively probe the role of other cell types, such as vascular endothelium, that are implicated in the vaso-occlusive process (*32*). Moreover, this work provides an impetus for the development of integrated chemical and biophysical indicators of disease that link multiple molecular and cellular pathways across diverse length and time scales. These tools could complement the growing biomolecular armamentarium for predicting clinical outcomes and revealing the mechanisms underlying human disease.

MATERIALS AND METHODS

Blood sample collection
Blood specimens were collected during the normal course of patient care at Massachusetts General Hospital and Brigham and Women's Hospital and used in experiments in accordance with a research protocol approved by the Partners Healthcare Institutional Review Board. Blood samples were collected in 5-ml EDTA vacutainers and stored at 4°C for up to 14 days. Hematocrit was determined with a Siemens ADVIA 2120 automated analyzer. Hemoglobin fractions were determined with cellulose agar electrophoresis and confirmed by high-performance liquid chromatography with a Tosoh G7 column. Blood samples used in simulated transfusion experiments were tested to exclude the presence of any RBC alloantibodies.

For all measurements, hematocrit was adjusted to 25% by fractionating RBCs and plasma in a centrifuge at 3500 rpm for 10 min. Separated plasma was then removed or added to adjust total hematocrit. For transfusion studies, hematocrit-adjusted sickle blood was mixed with type-matched HbA blood to achieve the desired sickle cell fraction. To treat with 5HMF (Sigma), we first dissolved 1 M of drug in dimethyl sulfoxide. Blood samples were treated with appropriate dose and incubated at 37°C for 1 hour. After incubation, samples were transferred to 4°C until ready for use.

Patient blood samples were classified as benign if all of the following criteria were met during the 12 months before sample collection and the 2 months after: no patient hospital admissions or emergency room visits for sickle cell disease–related complications, no blood transfusions for sickle cell disease–related indications, and no hydroxyurea use. Patient blood samples were classified as severe if the patient had had at least one hospital admission or emergency room visit for a sickle cell disease–related complication or a blood transfusion for a sickle cell disease–related indication in the 12 months before sample collection or the 2 months after.

Device fabrication
The device comprised three layers: the blood capillary, the gas reservoir, and a reservoir for hydration (Fig. 1A). Each of these layers was separated from the adjacent layers by a 100-μm-thick poly(dimethylsiloxane) (PDMS) membrane, which allowed for gas transport between the layers. The rectangular blood "capillary" was 7 cm long with a cross section that was 15 μm × 10 μm. The hydration layer, which was required to prevent dehydration of the blood through the membrane (*55*), was 30 cm long with a cross section that was 1.5 mm × 100 μm. The gas reservoir completely overlapped the hydration layer, but was 150 μm tall. The layers were fabricated in PDMS with soft lithography. The blood layer master was made by spinning SU-8 2015 (MicroChem Corp.) onto a silicon wafer at 3500 rpm for 30 s and then photocrosslinking the SU-8 through a 50,000-dpi (dots per inch) transparency mask. The hydration and gas layer molds were made by spinning SU-8 2050 at 1500 and 1000 rpm, respectively, for 30 s. The PDMS layers were assembled with thermal bonding. For the hydration layer and membrane, we mixed PDMS with a 20:1 elastomer/curing agent and spun this onto the mold at 500 rpm for 30 s. The gas layer was cast at 1-cm thickness with a 5:1 elastomer/curing agent and bonded to the hydration layer at 80°C for 2 hours. The blood layer and corresponding membrane was made by mixing PDMS with a 5:1 elastomer/curing agent and spin casting with the same conditions as for the hydration

layer. The gas and hydration reservoirs were then removed from the hydration layer mold and bonded to the blood layer at 80°C overnight. The final structure was then plasma-bonded to a glass microscope slide.

Device operation

The experimental setup is shown in Fig. 1. Gas was flowed through the top chamber of the device under constant pressure (1 psi) from precision pressure regulators (PRG200-25, Omega). We switched between 0% oxygen (N_2) and 21% oxygen (21% O_2, 5% CO_2, balance N_2) with solenoid valves downstream of the regulators. Phosphate-buffered saline (PBS) was flowed through the hydration layer at 1 ml/hour with a syringe pump. This aqueous layer prevented dehydration of the blood. Whole blood (EDTA-anticoagulated) from human patients was flowed through the capillary under constant pressure, provided by compressed N_2, with a digital pressure regulator (PCD, Alicat Scientific).

Oxygen measurement

Oxygen concentration of the gas phase was measured with a fiber optic sensor (FOXY, Ocean Optics) connected to the outlet of the gas reservoir. We also measured the oxygen saturation of the RBCs directly with an optical technique. An optical filter (Brightline 434 ± 17 nm, Semrock) was placed between the light source and the device (Fig. 1A). The transmission band of this filter was centered on 425 nm, in an absorption peak for deoxyhemoglobin (Fig. 1B). To confirm the validity of this gas-phase measurement as an estimate of the blood channel oxygen concentration, we measured oxygen concentration in the blood channel directly using an oxygen-sensitive luminescence probe (fig. S1). Tris(4,7-diphenyl-1,10-phenanthroline)ruthenium(II) dichloride complex (56) was dissolved in PBS at 1 mg/ml and flowed through the blood channel under the same conditions as the blood measurement. Luminescence was measured under illumination at 488 nm.

Blood conductance and dynamics

Blood rheology was measured by capturing high-speed videos in real time and performing video tracking of individual RBCs offline. Using this method, we were able to compute instantaneous blood velocities over very short time intervals and track changes in blood velocity as a function of RBC oxygenation state. Video processing methods were described in detail previously (40). Briefly, cells in each video frame were identified computationally on the basis of morphologic criteria. Cell locations in subsequent frames were linked to form trajectories with heuristics and machine learning techniques. We defined the velocity at each point in time as the median cell velocity calculated over a 32-frame video captured at higher than 200 fps. We excluded any noisy videos where the interquartile range (IQR) of calculated velocities was greater than the larger of the median velocity or 40 μm/s. All rheology data are reported as device conductance, which was calculated by dividing the median blood velocity by the applied pressure bias. Stretches of constant oxygen and pressure were identified automatically, and the beginning and ending of conductance transients were identified by examining a five-point moving average of the conductance. Once the time range was defined for a conductance transient, rates of conductance change were computed and fit to a linear function with the robust least-squares method available in the MATLAB curve fitting toolbox (MathWorks). Average rates of conductance change for each sample were defined by taking the mean of calculated transients from at least three independent deoxygenation cycles. Nonparametric analy-

sis to compare groups of samples was performed with the Mann-Whitney nonparametric test in the MATLAB statistics toolbox (57). Power analysis was performed with bootstrapping methods (resampling with replacement from our data set) along with numerically simulated trials (n = 100,000) (58).

Experiments flowing whole blood in microfluidic channels are prone to fouling, delamination, and other artifacts. We assessed the integrity of each deoxygenation/reoxygenation cycle by measuring the conductance before and after. Any significant change (>20%) likely reflected device compromise, and the results of such transients were excluded.

SUPPLEMENTARY MATERIALS

www.sciencetranslationalmedicine.org/cgi/content/full/4/123/123ra26/DC1
Fig. S1. Direct oxygen measurement in the blood channel.
Fig. S2. Metrics of sickle cell blood.
Table S1. Rates of conductance decrease from individual deoxygenation cycles for all patient samples (n = 29).
Movie S1. Vaso-occlusion and rescue in a microfluidic sickle cell disease model.

REFERENCES AND NOTES

1. E. M. Small, E. N. Olson, Pervasive roles of microRNAs in cardiovascular biology. *Nature* **469**, 336–342 (2011).
2. V. Brower, Biomarkers: Portents of malignancy. *Nature* **471**, S19–S21 (2011).
3. G. Miller, Alzheimer's biomarker initiative hits its stride. *Science* **326**, 386–389 (2009).
4. J. V. Bonventre, V. S. Vaidya, R. Schmouder, P. Feig, F. Dieterle, Next-generation biomarkers for detecting kidney toxicity. *Nat. Biotechnol.* **28**, 436–440 (2010).
5. M. L. Whitfield, L. K. George, G. D. Grant, C. M. Perou, Common markers of proliferation. *Nat. Rev. Cancer* **6**, 99–106 (2006).
6. D. G. Warnock, C. C. Peck, A roadmap for biomarker qualification. *Nat. Biotechnol.* **28**, 444–445 (2010).
7. A. N. Schechter, Hemoglobin research and the origins of molecular medicine. *Blood* **112**, 3927–3938 (2008).
8. M. H. Steinberg, R. P. Hebbel, Clinical diversity of sickle cell anemia: Genetic and cellular modulation of disease severity. *Am. J. Hematol.* **14**, 405–416 (1983).
9. G. M. Brittenham, A. N. Schechter, C. T. Noguchi, Hemoglobin S polymerization: Primary determinant of the hemolytic and clinical severity of the sickling syndromes. *Blood* **65**, 183–189 (1985).
10. O. S. Platt, B. D. Thorington, D. J. Brambilla, P. F. Milner, W. F. Rosse, E. Vichinsky, T. R. Kinney, Pain in sickle cell disease. Rates and risk factors. *N. Engl. J. Med.* **325**, 11–16 (1991).
11. R. K. Jain, K. Schlenger, M. Höckel, F. Yuan, Quantitative angiogenesis assays: Progress and problems. *Nat. Med.* **3**, 1203–1208 (1997).
12. L. S. Cohen, P. F. Escobar, C. Scharm, B. Glimco, D. A. Fishman, Three-dimensional power Doppler ultrasound improves the diagnostic accuracy for ovarian cancer prediction. *Gynecol. Oncol.* **82**, 40–48 (2001).
13. R. C. Wolf, G. Grön, F. Sambataro, N. Vasic, N. D. Wolf, P. A. Thomann, C. Saft, G. B. Landwehrmeyer, M. Orth, Magnetic resonance perfusion imaging of resting-state cerebral blood flow in preclinical Huntington's disease. *J. Cereb. Blood Flow Metab.* **31**, 1908–1918 (2011).
14. A. E. Karnoub, A. B. Dash, A. P. Vo, A. Sullivan, M. W. Brooks, G. W. Bell, A. L. Richardson, K. Polyak, R. Tubo, R. A. Weinberg, Mesenchymal stem cells within tumour stroma promote breast cancer metastasis. *Nature* **449**, 557–563 (2007).
15. C. L. Chaffer, R. A. Weinberg, A perspective on cancer cell metastasis. *Science* **331**, 1559–1564 (2011).
16. S. E. Cross, Y. S. Jin, J. Rao, J. K. Gimzewski, Nanomechanical analysis of cells from cancer patients. *Nat. Nanotechnol.* **2**, 780–783 (2007).
17. G. Y. Lee, C. T. Lim, Biomechanics approaches to studying human diseases. *Trends Biotechnol.* **25**, 111–118 (2007).
18. D. J. Weatherall, The inherited diseases of hemoglobin are an emerging global health burden. *Blood* **115**, 4331–4336 (2010).
19. S. K. Ballas, The cost of health care for patients with sickle cell disease. *Am. J. Hematol.* **84**, 320–322 (2009).
20. C. T. Noguchi, D. A. Torchi, A. N. Schechter, Determination of deoxyhemoglobin S polymer in sickle erythrocytes upon deoxygenation. *Proc. Natl. Acad. Sci. U.S.A.* **77**, 5487–5491 (1980).
21. W. A. Eaton, J. Hofrichter, Sickle cell hemoglobin polymerization. *Adv. Protein Chem.* **40**, 63–279 (1990).

22. M. H. Steinberg, Management of sickle cell disease. *N. Engl. J. Med.* **340**, 1021–1030 (1999).
23. S. H. Orkin, D. R. Higgs, Sickle cell disease at 100 years. *Science* **329**, 291–292 (2010).
24. M. T. Gladwin, R. J. Barst, O. L. Castro, V. R. Gordeuk, C. A. Hillery, G. J. Kato, D. B. Kim-Shapiro, R. Machado, C. R. Morris, M. H. Steinberg, E. P. Vichinsky, Pulmonary hypertension and NO in sickle cell. *Blood* **116**, 852–854 (2010).
25. H. F. Bunn, Pathogenesis and treatment of sickle cell disease. *N. Engl. J. Med.* **337**, 762–769 (1997).
26. M. H. Steinberg, Sickle cell anemia, the first molecular disease: Overview of molecular etiology, pathophysiology, and therapeutic approaches. *ScientificWorldJournal* **8**, 1295–1324 (2008).
27. S. K. Ballas, N. Mohandas, Sickle red cell microrheology and sickle blood rheology. *Microcirculation* **11**, 209–225 (2004).
28. H. Hiruma, C. T. Noguchi, N. Uyesaka, A. N. Schechter, G. P. Rodgers, Contributions of sickle hemoglobin polymer and sickle cell membranes to impaired filterability. *Am. J. Physiol.* **268**, H2003–H2008 (1995).
29. S. Chien, A. A. Kaperonis, R. G. King, H. H. Lipowsky, E. A. Schmalzer, L. A. Sung, K. L. Sung, S. Usami, Rheology of sickle cells and its role in microcirculatory dynamics. *Prog. Clin. Biol. Res.* **240**, 151–165 (1987).
30. G. B. Nash, C. S. Johnson, H. J. Meiselman, Rheologic impairment of sickle RBCs induced by repetitive cycles of deoxygenation-reoxygenation. *Blood* **72**, 539–545 (1988).
31. W. A. Eaton, J. Hofrichter, Hemoglobin S gelation and sickle cell disease. *Blood* **70**, 1245–1266 (1987).
32. M. Tsai, A. Kita, J. Leach, R. Rounsevell, J. N. Huang, J. Moake, R. E. Ware, D. A. Fletcher, W. A. Lam, In vitro modeling of the microvascular occlusion and thrombosis that occur in hematologic diseases using microfluidic technology. *J. Clin. Invest.* **122**, 408–418 (2012).
33. K. T. McDonagh, G. J. Dover, R. E. Donahue, D. G. Nathan, B. Agricola, E. Byrne, A. W. Nienhuis, Hydroxyurea-induced HbF production in anemic primates: Augmentation by erythropoietin, hematopoietic growth factors, and sodium butyrate. *Exp. Hematol.* **20**, 1156–1164 (1992).
34. S. H. Embury, The not-so-simple process of sickle cell vasoocclusion. *Microcirculation* **11**, 101–113 (2004).
35. R. Adams, V. McKie, F. Nichols, E. Carl, D. L. Zhang, K. McKie, R. Figueroa, M. Litaker, W. Thompson, D. Hess, The use of transcranial ultrasonography to predict stroke in sickle cell disease. *N. Engl. J. Med.* **326**, 605–610 (1992).
36. R. J. Adams, V. C. McKie, L. Hsu, B. Files, E. Vichinsky, C. Pegelow, M. Abboud, D. Gallagher, A. Kutlar, F. T. Nichols, D. R. Bonds, D. Brambilla, G. Woods, N. Olivieri, C. Driscoll, S. Miller, W. Wang, A. Hurlett, C. Scher, B. Berman, E. Carl, A. M. Jones, E. S. Roach, E. Wright, R. A. Zimmerman, M. Waclawiw, Prevention of a first stroke by transfusions in children with sickle cell anemia and abnormal results on transcranial Doppler ultrasonography. *N. Engl. J. Med.* **339**, 5–11 (1998).
37. R. J. Adams, D. Brambilla; Optimizing Primary Stoke Prevention in Sickle Cell Anemia (STOP 2) Trial Investigators, Discontinuing prophylactic transfusions used to prevent stroke in sickle cell disease. *N. Engl. J. Med.* **353**, 2769–2778 (2005).
38. G. A. Barabino, M. O. Platt, D. K. Kaul, Sickle cell biomechanics. *Annu. Rev. Biomed. Eng.* **12**, 345–367 (2010).
39. J. M. Higgins, D. T. Eddington, S. N. Bhatia, L. Mahadevan, Sickle cell vasoocclusion and rescue in a microfluidic device. *Proc. Natl. Acad. Sci. U.S.A.* **104**, 20496–20500 (2007).
40. J. M. Higgins, D. T. Eddington, S. N. Bhatia, L. Mahadevan, Statistical dynamics of flowing red blood cells by morphological image processing. *PLoS Comput. Biol.* **5**, e1000288 (2009).
41. Z. Zhujun, W. R. Seitz, Optical sensor for oxygen based on immobilized hemoglobin. *Anal. Chem.* **58**, 220–222 (1986).
42. P. K. Kundu, I. M. Cohen, *Fluid Mechanics* (Elsevier, New York, ed. 3, 2004), pp. 279–285.
43. H. H. Lipowsky, Microvascular rheology and hemodynamics. *Microcirculation* **12**, 5–15 (2005).
44. M. H. Zweig, G. Campbell, Receiver-operating characteristic (ROC) plots: A fundamental evaluation tool in clinical medicine. *Clin. Chem.* **39**, 561–577 (1993).
45. I. Akinsheye, A. Alsultan, N. Solovieff, D. Ngo, C. T. Baldwin, P. Sebastiani, D. H. K. Chui, M. H. Steinberg, Fetal hemoglobin in sickle cell anemia. *Blood* **118**, 19–27 (2011).
46. L. A. Verduzco, D. G. Nathan, Sickle cell disease and stroke. *Blood* **114**, 5117–5125 (2009).
47. O. Abdulmalik, M. K. Safo, Q. Chen, J. Yang, C. Brugnara, K. Ohene-Frempong, D. J. Abraham, T. Asakura, 5-Hydroxymethyl-2-furfural modifies intracellular sickle haemoglobin and inhibits sickling of red blood cells. *Br. J. Haematol.* **128**, 552–561 (2005).
48. J. B. Haun, C. M. Castro, R. Wang, V. M. Peterson, B. S. Marinelli, H. Lee, R. Weissleder, Micro-NMR for rapid molecular analysis of human tumor samples. *Sci. Transl. Med.* **3**, 71ra16 (2011).
49. V. S. Vaidya, J. S. Ozer, F. Dieterle, F. B. Collings, V. Ramirez, S. Troth, N. Muniappa, D. Thudium, D. Gerhold, D. J. Holder, N. A. Bobadilla, E. Marrer, E. Perentes, A. Cordier, J. Vonderscher, G. Maurer, P. L. Goering, F. D. Sistare, J. V. Bonventre, Kidney injury molecule-1 outperforms traditional biomarkers of kidney injury in preclinical biomarker qualification studies. *Nat. Biotechnol.* **28**, 478–485 (2010).
50. X. W. van den Tweel, J. H. van der Lee, H. Heijboer, M. Peters, K. Fijnvandraat, Development and validation of a pediatric severity index for sickle cell patients. *Am. J. Hematol.* **85**, 746–751 (2010).
51. E. C. Klatt, V. Kumar, *Robbins and Cotran Review of Pathology* (Saunders/Elsevier, New York, ed. 3, 2009).
52. M. de Montalembert, Hydroxyurea treatment in patients affected with sickle cell anemia: Efficacy and safety. *Transfus. Clin. Biol.* **15**, 34–38 (2008).
53. G. R. Serjeant, B. E. Serjeant, K. P. Mason, I. R. Hambleton, C. Fisher, D. R. Higgs, The changing face of homozygous sickle cell disease: 102 patients over 60 years. *Int. J. Lab. Hematol.* **31**, 585–596 (2009).
54. D. G. Nathan, Search for improved therapy of sickle cell anemia. *J. Pediatr. Hematol. Oncol.* **24**, 700–703 (2002).
55. X. Noblin, L. Mahadevan, I. A. Coomaraswamy, D. A. Weitz, N. M. Holbrook, M. A. Zwieniecki, Optimal vein density in artificial and real leaves. *Proc. Natl. Acad. Sci. U.S.A.* **105**, 9140–9144 (2008).
56. I. Klimant, O. S. Wolfbeis, Oxygen-sensitive luminescent materials based on silicone-soluble ruthenium diimine complexes. *Anal. Chem.* **67**, 3160–3166 (1995).
57. M. Hollander, D. A. Wolfe, *Nonparametric Statistical Methods* (John Wiley & Sons, Hoboken, NJ, 1999).
58. T. Hesterberg, S. Monaghan, D. S. Moore, A. Clipson, R. Epstein, Bootstrap methods and permutation tests, in *Introduction to the Practice of Statistics*, D. S. Moore, G. P. McCabe, Eds. (W. H. Freeman & Co., New York, ed. 5, 2005).

Citation: D. K. Wood, A. Soriano, L. Mahadevan, J. M. Higgins, S. N. Bhatia, A biophysical indicator of vaso-occlusive risk in sickle cell disease. *Sci. Transl. Med.* **4**, 123ra26 (2012).

Supplementary Materials for

A Biophysical Indicator of Vaso-occlusive Risk in Sickle Cell Disease

David K. Wood, Alicia Soriano, L. Mahadevan,* John M. Higgins,* Sangeeta N. Bhatia

*To whom correspondence should be addressed. E-mail: lm@seas.harvard.edu (L.M.);
john_higgins@hms.harvard.edu (J.M.H.)

This PDF file includes:

Other Supplementary Material for this manuscript includes the following:
(available at www.sciencetranslationalmedicine.org/cgi/content/full/4/123/123ra26/DC1)
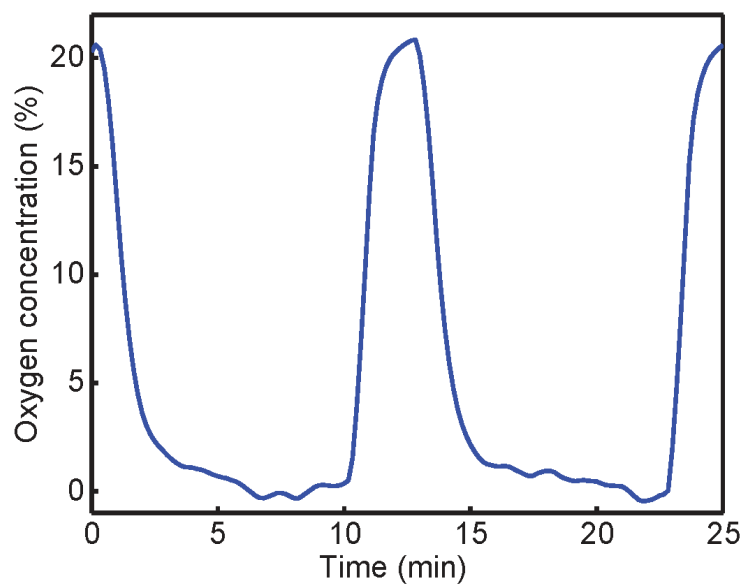
Figure S1. Direct oxygen measurement in the blood channel. Luminescent dye Tris(4,7-diphenyl-1,10-phenanthroline)ruthenium(II) dichloride was dissolved in buffer and flowed through the blood channel (in the absence of blood) of the microfluidic device. Oxygen concentration was measured based on luminescence intensity.
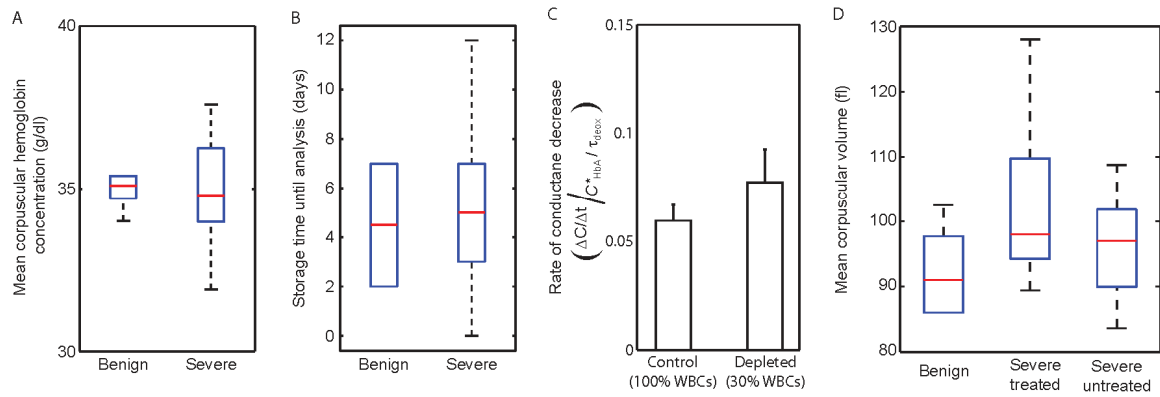
Figure S2. Metrics of sickle cell blood. (**A** to **B**) Box plots comparing mean corpuscular hemoglobin concentration (MCHC) (A) and sample storage time (B) for benign ($n = 6$) and severe ($n = 23$) samples. (**C**) Mean rate of conductance decrease and standard deviation for a sample before and after depletion of the WBCs. (**D**) Box plot comparing mean corpuscular volume (MCV) for benign ($n = 6$), treated severe ($n = 12$), and untreated severe samples ($n = 11$). In the box plots, the red line is the median, the blue box shows interquartile range (IQR), and the dashed lines show extent of data within 1.5-fold IQR. All conductance values were scaled by the mean HbA blood conductance [~1.7 μm/s/mmHg (0.013 μm/s/Pa)].

Table S1. Rates of conductance decrease from individual deoxygenation cycles for all patient samples (*n* = 29). Rates of conductance decrease are shown for each independent deoxygenation trial as well as overall means and standard deviations shown in Fig. 4. Rates of conductance decrease are scaled by mean HbA blood conductance [~1.7 μm/s/mmHg (0.013 μm/s/Pa)] divided by the time scale for hemoglobin deoxygenation (~10 s).

Clinical Status	Rate of Conductance Decrease from Individual De-Oxygenation Cycles $((\Delta C/\Delta t)/(C^*_{HbA}/\tau_{deox}))$														Mean	Standard Deviation
Benign	0.0289	0.0264	0.0497	0.0336	0.0317										0.0341	0.0092
Benign	0.0326	0.0371	0.0474	0.0353	0.0367	0.0249									0.0357	0.0073
Benign	0.0002	0.0066	0.0014	0.0006	0.0324										0.0082	0.0138
Benign	0.0616	0.0631	0.0563	0.0357	0.0683										0.0570	0.0126
Benign	0.0330	0.0625	0.0254												0.0403	0.0196
Benign	0.0726	0.0763	0.0676	0.0577	0.0668										0.0682	0.0070
Treated Severe	0.1534	0.1243	0.0957	0.1008	0.0973	0.0971									0.1114	0.0232
Treated Severe	0.1340	0.1324	0.1109	0.1365	0.1550	0.1501	0.1355	0.1693	0.1115	0.0610	0.0942	0.0852	0.1264	0.0650	0.1191	0.0328
Treated Severe	0.0518	0.0856	0.0600	0.0416	0.0250	0.0678	0.1763								0.0726	0.0496
Treated Severe	0.1897	0.2262	0.2033	0.1843	0.2130	0.1373	0.1505	0.1713							0.1844	0.0305
Treated Severe	0.0583	0.0324	0.0425	0.0750	0.0542	0.0241									0.0477	0.0185
Treated Severe	0.0287	0.0513	0.0320												0.0373	0.0122
Treated Severe	0.1487	0.1379	0.1204	0.1179	0.1083										0.1266	0.0163
Treated Severe	0.2052	0.1412	0.1035												0.1500	0.0514
Treated Severe	0.0920	0.0965	0.0460	0.0773	0.0656										0.0755	0.0205
Treated Severe	0.1142	0.1322	0.1107	0.1181	0.1249										0.1200	0.0086
Untreated Severe	0.1085	0.1041	0.0718	0.0841	0.0889										0.0915	0.0150
Untreated Severe	0.0713	0.0452	0.0658	0.0817	0.0235										0.0575	0.0232
Untreated Severe	0.0946	0.0895	0.0728	0.0792	0.0854										0.0843	0.0085
Untreated Severe	0.1666	0.1804	0.1190	0.1283	0.1291										0.1447	0.0270
Untreated Severe	0.1072	0.1056	0.1179	0.0796	0.0950	0.0932									0.0997	0.0133
Untreated Severe	0.1012	0.1177	0.0437	0.1035	0.0427	0.0596									0.0781	0.0332
Untreated Severe	0.0326	0.0260	0.0039	0.0161	0.0068	0.0210	0.0183								0.0178	0.0101
Untreated Severe	0.0872	0.0726	0.0819	0.0928	0.0652	0.0656	0.0950								0.0801	0.0124
Untreated Severe	0.0291	0.0334	0.0289	0.0383	0.0423	0.0227									0.0325	0.0071
Untreated Severe	0.1099	0.0868	0.1136	0.1223	0.0837										0.1033	0.0171
Untreated Severe	0.1643	0.2291	0.1357	0.2280	0.1495	0.1720									0.1798	0.0398
Untreated Severe	0.0039	0.0256	0.0227	0.0184	0.0196	0.0243									0.0191	0.0079
Untreated Severe	0.1423	0.1066	0.1068	0.1227	0.1101										0.1177	0.0153

Movie S1. Vaso-occlusion and rescue in a microfluidic sickle cell disease model. The movie begins with nitrogen in the gas reservoir. As the cells were deoxygenated, they stiffened and changed morphology to a sickle shape, with blood flow slowing almost completely. Air was reintroduced into the gas reservoir, allowing the hemoglobin to re-oxygenate. As the hemoglobin polymers melted, the cells softened, and flow resumed, eventually returning to pre-occlusion velocity. Constant pressure bias was maintained in the blood channel during the entire (de)oxygenation cycle.